Supplementary Information

Impact of Carbon Impurities on Air Stability of MOCVD 2D-MoS_2

*Amir Ghiami, [1, *] Annika Grundmann, [1] Songyao Tang, [1] Hleb Fiadziushkin, [1] Zhaodong Wang, [2, 3] Stephan Aussen, [2] Susanne Hoffmann-Eifert, [2] Michael Heuken, [1, 4] Holger Kalisch, [1] and Andrei Vescan [1]*

[1] Compound Semiconductor Technology, RWTH Aachen University, Sommerfeldstraße 18, 52074 Aachen, Germany
[2] Peter-Grünberg-Institute (PGI 7/10) and JARA-FIT, Forschungszentrum Jülich GmbH, 52425 Jülich, Germany
[3] Faculty of Georesources and Materials Engineering, RWTH Aachen University, Intzestr. 1, 52072 Aachen, Germany
[4] AIXTRON SE, Dornkaulstr. 2, 52134 Herzogenrath, Germany

Corresponding Author:

* Email: ghiami@cst.rwth-aachen.de

SEM and XPS analyses, complementary results. Surface coverage of multiple as-deposited samples from each run were analyzed using the ImageJ software. ML, BL and TL coverages are given in Figure S1.

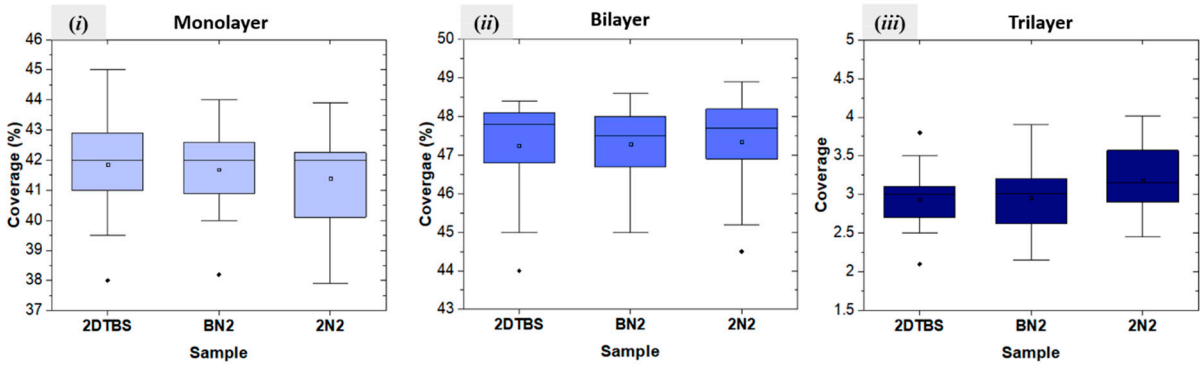

Figure S1. Extended SEM analyses of as-deposited layers: calculated ML, BL and TL coverage of multiple samples using ImageJ

High-resolution fitted Mo3d-S2s and S2p core levels show the formation of pure MoS_2, and the small variations in the S/Mo stoichiometry values discussed in section 3.1 of the main article are not detectable in the core level line shapes. (Figure S1-a)

Regarding the XPS peaks calibration, since the carbon peaks detected in as-deposited 2D-MoS_2 samples are not dominated by adventitious carbon, they cannot be used as a reference for the calibration of the peaks. For this reason, an XPS measurement on a bare sapphire wafer (as also used for MOVCD) was performed to obtain the calibrated Al2p peak position. This value could be used as a calibration reference for the peaks in MOCVD samples. The high-resolution C1s and Al2p core levels of the bare sapphire are given in Figure S2-b *(i)-(ii)*. The binding energy of the C1s and Al2p peaks are found to be 284.24 and 73.41 eV, respectively.

The detected carbon peak is unambiguously attributed to adventitious carbon. Then, the calibration for binding energies was carried out for the main C1s peak at 284.80 eV. [1] Accordingly, the Al2p peak was found to be at 73.97 eV. The obtained calibrated binding energy for the Al2p peak was then used as the reference to calibrate the XPS peaks of as-deposited MOCVD 2D-MoS_2.

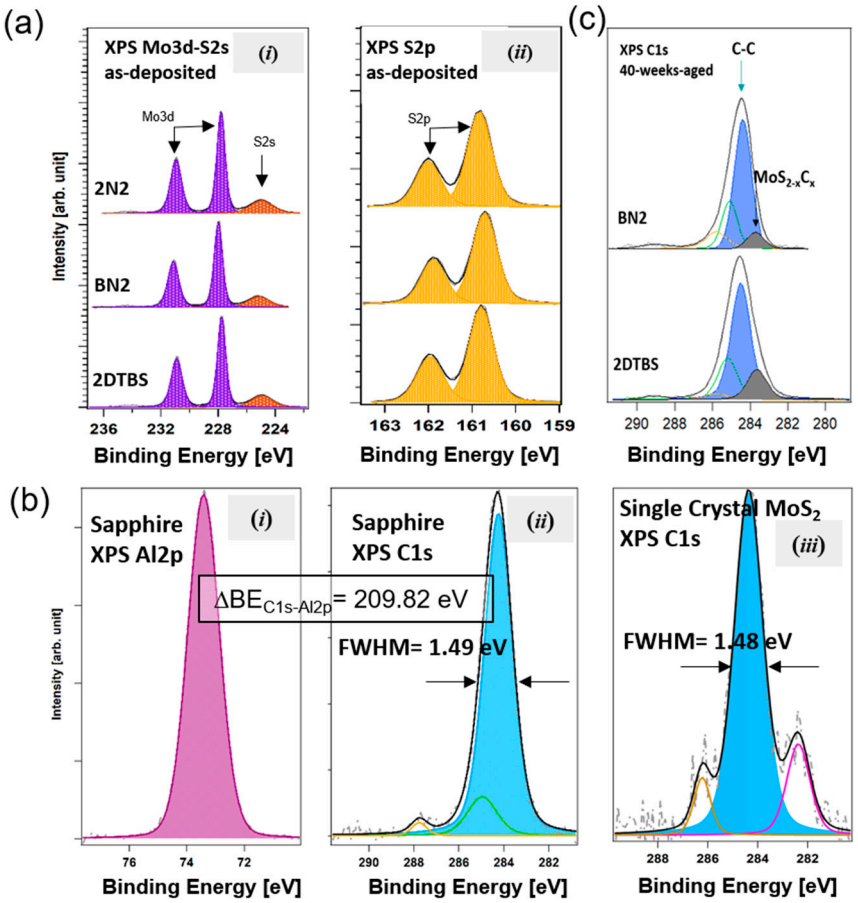

Figure S2. Fitted high-resolution (a) Mo3d-S2s *(i)* and S2p *(ii)* core levels of as-deposited samples, (b) Al2p *(i)* and C1s *(ii)* core levels of bare sapphire and C1s core level of single-crystal MoS_2 *(iii)*, (c) C1s core levels of 40-weeks-aged 2DBS and BN2 samples.

The carbon C1s XPS peak of single crystal MoS_2 is also shown in Figure S2-b (iii); the FWHM of the peak can be taken as the typical FWHM value of adventitious carbon on MoS_2.

Figure S2-c shows the XPS C1s high-resolution fitted spectra of 40-weeks-aged 2DTBS and BN2 samples, which contain 12 and 7 atom. % of carbide species, respectively.

The XPS O1s core levels of as-deposited, 20-weeks- and 40-weeks-aged layers are illustrated in Figure S3 a. For all three samples, the lineshape demonstrates the evolution of a shoulder peak (in red rectangle) towards higher binding energies than the main peak (in the grey rectangle). The main peak is associated with aluminum oxide signals from sapphire substrate, while the newly emerged shoulder peak can be attributed to additional organic C-O or C=O bonds from the atmosphere or the formation of metal carbonate [2], [3]. Notably, the XPS O1s peak does not indicate the formation of any molybdenum oxide, because it would have appeared as a shoulder peak at lower binding energies relative to the O1s main peak in the grey rectangle.

Additionally, SEM images of the 40-weeks-aged layers are shown in Figure S3 b. These layers do not exhibit severe degradation or cracking, unlike some other works reported literature [4], [5].

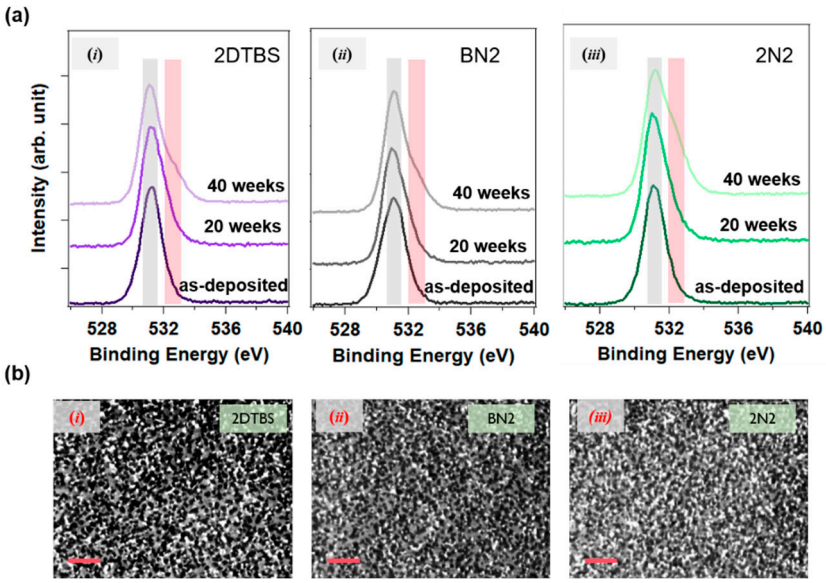

Figure S3. (a) High-resolution XPS O1s core levels of as-deposited, 20-weeks- and 40-weeks-aged layers, (b) SEM pictures of 40-weeks-aged layers. The scalebar is equal to 500 nm.

µ-Raman of as-deposited samples. The extended Raman spectra of the three as-deposited samples are shown in Figure S4. The two characteristic Raman peaks of MoS_2, namely, $E_{2g}{}^1$ and A_{1g}, were detected for all three samples at ~382 cm^{-1} and 407 cm^{-1}, respectively. In MOCVD TMDC layers, the detection of the carbon peak has been reported in many other works; the D and G bands were found to be at ~1360 and ~1590 cm^{-1}.[6]–[8] However, as shown in Figure S3, no carbon peak could be recorded in the as-deposited samples in this work, which is an indication of well optimized MOCVD processes. Moreover, combining these results with those of the XPS investigation suggests that the level of carbon concentration is low enough not to be detected by Raman characterization, and a more sensitive technique (i.e. XPS in this work) is required to probe the incorporation of carbon in the 2D structure.

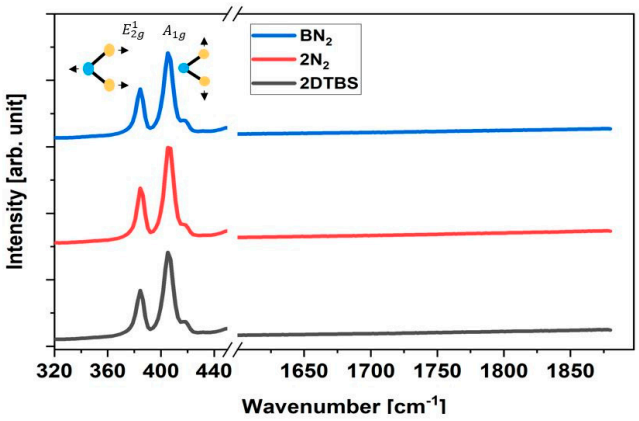

Figure S3. Extended µ-Raman spectra of as-deposited samples

Photoluminescence statistical analysis. The distributions of the A exciton PL intensity maps shown in Figure 1-b are depicted in the histograms in Figure S5.

To obtain the average values of the PL intensities reported in Table 1, a Gaussian distribution function was fitted to the histograms. Then, the center of the fitted curves was calculated, reported as X_c in Figure S4.

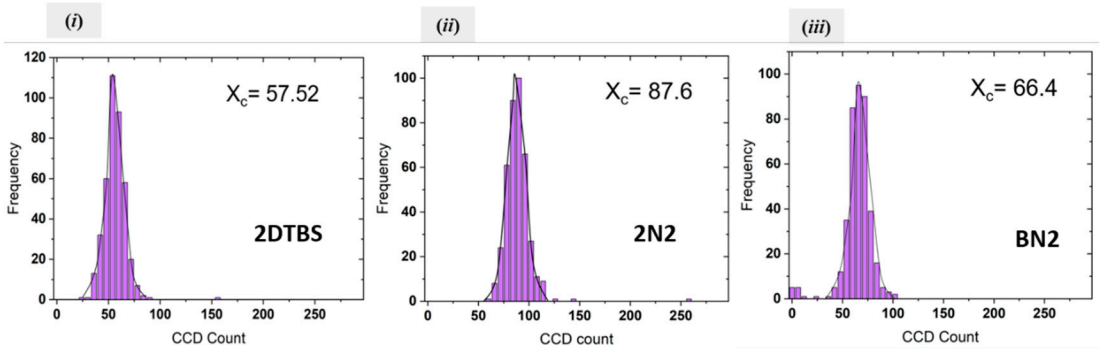

Figure S4. Distribution of A^0 PL intensity, obtained from the PL maps given in Figure 3

References

[1] H. Cun *et al.*, "Wafer-scale MOCVD growth of monolayer MoS_2 on sapphire and SiO_2," *Nano Res.*, vol. 12, no. 10, pp. 2646–2652, Oct. 2019, doi: 10.1007/s12274-019-2502-9.

[2] S. Gredelj, A. R. Gerson, S. Kumar, and G. P. Cavallaro, "Characterization of aluminium surfaces with and without plasma nitriding by X-ray photoelectron spectroscopy," *Appl. Surf. Sci.*, vol. 174, no. 3–4, pp. 240–250, 2001, doi: 10.1016/S0169-4332(01)00169-6.

[3] K. Xie *et al.*, "Superior Potassium Ion Storage via Vertical MoS_2 'Nano-Rose' with Expanded Interlayers on Graphene," *Small*, vol. 13, no. 42, p. 1701471, Nov. 2017, doi: 10.1002/smll.201701471.

[4] J. Gao, B. Li, J. Tan, P. Chow, T. M. Lu, and N. Koratkar, "Aging of Transition Metal Dichalcogenide Monolayers," *ACS Nano*, vol. 10, no. 2, pp. 2628–2635, 2016, doi: 10.1021/acsnano.5b07677.

[5] K. Yao *et al.*, "Growth of Monolayer MoS_2 on Hydrophobic Substrates as a Novel and Feasible Method to Prevent the Ambient Degradation of Monolayer MoS_2," *MRS Adv.*, vol. 5, no. 52–53, pp. 2707–2715, Nov. 2020, doi: 10.1557/adv.2020.292.

[6] C. M. Schaefer *et al.*, "Carbon Incorporation in MOCVD of MoS_2 Thin Films Grown from an Organosulfide Precursor," *Chem. Mater.*, 2021, doi: 10.1021/acs.chemmater.1c00646.

[7] A. Grundmann *et al.*, "H_2S-free Metal-Organic Vapor Phase Epitaxy of Coalesced 2D WS_2 Layers on Sapphire," *MRS Adv.*, vol. 4, no. 10, pp. e1–e1, Sep. 2019, doi: 10.1557/adv.2019.229.

[8] M. Marx *et al.*, “Metalorganic Vapor-Phase Epitaxy Growth Parameters for Two-Dimensional MoS_2,” *J. Electron. Mater.*, vol. 47, no. 2, pp. 910–916, Feb. 2018, doi: 10.1007/s11664-017-5937-3.